The Cryosphere Discuss., 8, 2375–2401, 2014
www.the-cryosphere-discuss.net/8/2375/2014/
doi:10.5194/tcd-8-2375-2014

The Cryosphere
Discussions
Open Access

Changes in Imja Tsho in the Mt. Everest region of Nepal

M. A. Somos-Valenzuela[1], **D. C. McKinney**[1], **D. R. Rounce**[1], **and A. C. Byers**[2]

[1]Center for Research in Water Resources, University of Texas at Austin, Austin, Texas, USA
[2]The Mountain Institute, Washington DC, USA

Received: 2 April 2014 – Accepted: 23 April 2014 – Published: 8 May 2014

Correspondence to: D. C. McKinney (daene@aol.com)

Published by Copernicus Publications on behalf of the European Geosciences Union.

Title Page
Abstract | Introduction
Conclusions | References
Tables | Figures
|◀ | ▶|
◀ | ▶
Back | Close
Full Screen / Esc
Printer-friendly Version
Interactive Discussion

Abstract

Imja Tsho, located in the Sagarmatha (Everest) National Park of Nepal, is one of the most studied and rapidly growing lakes in the Himalayan range. Compared with previous studies, the results of our sonar bathymetric survey conducted in September 2012 suggest that the maximum depth has increased from 98 m to 116 ± 0.25 m since 2002, and that its estimated volume has grown from 35.8 ± 0.7 million m^3 to 61.6 ± 1.8 million m^3. Most of the expansion of the lake in recent years has taken place in the glacier terminus–lake interface on the eastern end of the lake, with the glacier receding at about 52.6 ± 0.3 m yr^{-1} and the lake expanding in area by 0.039 ± 0.0195 km^2 yr^{-1}. A ground penetrating radar survey of the Imja-Lhotse Shar glacier just behind the glacier terminus shows that the ice is over 217 ± 12.71 m thick in the center of the glacier. The volume of water that could be released from the lake in the event of a breach in the damming moraine on the western end of the lake has increased from 21 million m^3 in 2002 to 34.8 ± 0.54 million m^3 in 2012.

1 Introduction

The formation of glacial lakes in the Nepal Himalaya has been increasing since the early 1960s (Gardelle et al., 2011). Twenty-four new glacial lakes have formed, and 34 have grown substantially in the Sagarmatha (Mt. Everest) and Makalu-Barun National Parks of Nepal during the past several decades (Bajracharya et al., 2007). Accompanying this increase in the number and size of glacial lakes is an associated increase in the risk of glacial lake outburst flood (GLOF) events (Ives et al., 2010; Shrestha and Aryal, 2011). At least twelve of the new or growing lakes within the Dudh Koshi watershed of this region may be of concern based on their rapid growth as evidenced by comparative time lapse, remotely sensed imagery over the past several decades (Bajracharya et al., 2007; Jianchu et al., 2007; Bolch et al., 2008; Watanabe et al., 2009).

GLOFs are the sudden release of a large amount of glacial lake water into a downstream watercourse, many orders of magnitude higher than the normal flow due to the of a moraine damming the lake (Carrivick and Rushmer, 2006). They can cause severe damage to downstream communities, infrastructure, agriculture, economic activities, and landscapes because of the sheer magnitude and power of the flood and debris flows produced (Bajracharya et al., 2007). The Khumbu region of Nepal (Fig. 1) is often mentioned as an area prone to GLOF events. The appearance and possible danger posed by new glacial lakes in this region has prompted national and regional groups to begin assessing methods to mitigate increasing GLOF risks to communities, infrastructure, and landscapes downstream of the lakes (e.g., UNDP, 2013).

The Imja-Lhotse Shar glacier is located in the Imja Khola watershed in the Khumbu region, about 9 km south of the summit of Mt. Everest. It is comprised of the Lhotse Shar glacier to the north and the Imja glacier to the east. The Amphu glacier to the south appears to no longer contribute to the Imja-Lhotse Shar glacier. Bolch et al. (2011) studied the mass change for ten glaciers in the Khumbu region south and west of Mt. Everest, and found that the Imja-Lhotse Shar glacier exhibited the largest loss rate in the Khumbu region, $-0.5 \pm 0.09\,\mathrm{m.w.e.\,yr^{-1}}$ (meter of water equivalent per year) for the period 1970–2007. Nuimura et al. (2012) also report significant surface lowering of the glaciers of this area, including $-0.81 \pm 0.22\,\mathrm{m.w.e.\,yr^{-1}}$ (1992–2008) for the Imja-Lhotse Shar glacier.

Hammond (1988), in one of the first studies in the region concerned with glacial lakes, identified twenty-four lakes and numerous other melt water ponds in the Khumbu region in 1988. Most of these lakes began forming in the late 1950s to early 1960s, and have expanded considerably since then, especially Imja Tsho (lake). For example, the 1963 Schneider map of the Everest region does not show a lake on the Imja-Lhotse Shar glacier, but rather five small melt water ponds on the surface near the glacier’s terminus (Hagen et al., 1963). The expansion of Imja Tsho since the mid-1950s has been documented through the use of repeat photography (Byers, 2007) and remote sensing (Mool et al., 2001).

The lake is bounded to the east by the Imja-Lhotse Shar glacier, to the north and south by lateral moraines, and to the west by the moraine of the former glacier terminus. The troughs formed alongside the lateral moraines act as gutters, trapping debris derived from rockfall, snow avalanches, and fluvial transport (Hambrey et al., 2008). Imja Tsho is dammed by a 700 m wide by 700 m long, ice-cored, debris-covered, former glacier tongue through which water exits by means of an outlet lake complex (Watanabe et al., 2009). The former glacier tongue still contains ice as evidenced by outcrops of bare ice, ponds formed by melt water from ice in the moraine, traces of old ponds (Yamada and Sharma, 1993). The incision of the outlet channel complex has lowered the lake level by some 37 m over the last four decades (Watanabe et al., 2009; Lamsal et al., 2011). The discharge from the lake forms the river Imja Khola (small river), which is a tributary of the Dudh Koshi river. It is likely that the outlet complex is evolving into a new arm of the lake (Benn et al., 2012). Portions of the bottom of Imja Tsho are most likely ice, given the observed frequency of subaqueous calving and the presence of icebergs with apparent subaqueous origins, and the presumed melting of this ice has caused the lake level to fall for several decades (Watanabe et al., 1995; Fujita et al., 2009).

We conducted a sonar bathymetric survey of Imja Tsho and a ground penetrating radar (GPR) survey of the Imja-Lhotse Shar glacier in September 2012. The purpose of this paper is to report on the results of those surveys and examine the changes in Imja Tsho volume and area.

2 Method

2.1 Bathymetric survey

Previous bathymetric surveys of Imja Tsho were conducted in 1992 (Yamada and Sharma, 1993) and 2002 (Sakai et al., 2003; Fujita et al., 2009). Measurements were taken at 61 points around the lake in 1962 through holes drilled in the ice and, in 2002 at 80 uniformly spaced points on the lake, both using a weighted line technique. We conducted a bathymetric survey of Imja Tsho during 22–24 September 2012 using a Biosonic Habitat EchoSounder MX sonar unit mounted on an inflatable raft. The sonar unit has an accuracy of 2.7 cm ± 0.2 % of depth and a maximum depth of operation of 100 m with the available transducer. Several transects were made around the lake with the sonar unit measuring the depth (Fig. 2).

For areas with depths greater than 100 m where the equipment could not measure depth it did record the position of those points. To estimate the depth of the lake in these areas, interpolation was made with values of the shallower, measured points by establishing transects crossing the lake from north to south over these deep areas. The lake bottom shape along these transects is assumed to be parabolic fit and an interpolation is fit to the measured points and used to estimate the depths at the missing points.

During the survey, large icebergs blocked access to the eastern end of the lake, so interpolation was used to fill in missing values in this area. Robertson et al. (2012) found that ice ramps at the glacier end of glacial lakes tend to have slopes 11–30° and exhibit subaqueous calving. To fill in the missing values, we assume that the lake bottom in the eastern part of the lake is comprised of an ice ramp sloping up toward the glacier terminus and that the ice ramp has a slope of 10–30° in the first 150 m near the glacier; 10–20° in the next 150 m, and 2–5° until the measured points are reached. Three transects, north to south, at 150, 300 and 450 m from the eastern shoreline with the shape of the eastern-most measured transect are used for interpolation. The lake depth at the points along the three lines were calculated so that they agree with the slopes described by Robertson et al. (2012). Since these slopes have maximum and a minimum values, each point along these lines also has a maximum and a minimum value as well that can be used in the uncertainty calculations described below.

In calculating the uncertainty associated with the lake volume, we consider the uncertainty in the depth measurements, and the uncertainty in the slope of the ice ramp, but not the uncertainty in the lake area. The uncertainty of the lake volume calculations are estimated using a range of depth for each point that was interpolated in areas deeper than 100 m or estimated from ice ramp slopes on the eastern end of the lake. In the areas where the depth of the lake was measured with the sonar device, we could directly calculate the maximum and minimum values using the error of the equipment. For points in areas deeper than 100 m that were interpolated, maximum and minimum depth values were calculated on 5 m raster files, thus providing two values for each 25 m^2. Using the points that were either measured, interpolated in areas deeper than 100 m or estimated using ice ramp slopes, two 5 m resolution raster files were generated, one for the maximum depth and one for the minimum depth. Thus, each point has two values representing the maximum and minimum depth for each cell of 25 m^2. We assume that the depth in each cell follows a uniform probability distribution (USACE, 2003), so that any depth within the maximum to minimum depth range has an equal probability of being the actual depth of the cell. In order to calculate the volume of the lake we used a Monte Carlo simulation with 2000 samples, which allows us to include the uncertainty in our measurement and assumptions; and calculate the expected value and standard deviation of the water volume.

2.2 Lake area calculation

Bathymetric surveys of Imja Tsho conducted in April 1992 (Yamada and Sharma, 1993), April 2002 (Sakai et al., 2003), and September 2012 (this study) are compared here. Landsat satellite imagery is used to compare the areal expansion of Imja Tsho with the changes in bathymetry. Unfortunately, Landsat images from the exact dates of the bathymetric surveys are not available, so the images selected are as close to the survey dates as possible. The images comprise a Landsat-4 image from 4 July 1992 and Landsat-7 images from 4 October 2002 and 29 September 2012. The processing level of the Landsat images are all L1T, indicating that the images are all geometrically rectified using ground control points from the 2005 Global Land Survey in conjunction with the 90 m Shuttle Radar Topographic Mission (SRTM) global DEM. The swipe visualization tool in PCI Geomatica 2013 was used with Landsat band 7 from each image to confirm that the images were properly co-registered. The co-registered images were used to compute changes in the areal extent of Imja Tsho.

The normalized differential water index (NDWI) was used to semi-automatically compute the area of the lake. Previous studies have computed the NDWI using NIR and Blue bands (Huggel et al., 2002; Bolch et al., 2008) or the NIR and Green bands (McFeeters, 1996). Frey et al. (2010) used a combination of the NDWI computed with the NIR and Blue band along with the ratio of the NIR and SWIR bands to delineate glacial lakes in the Swiss Alps. This study tested computing the NDWI with several different band combinations (e.g., Blue, NIR, SWIR) with the aim of identifying a single band combination and a threshold value that could be applied to the three Landsat images to precisely delineate Imja Tsho. The NDWI using the NIR (Band 4) and SWIR (Band 5) bands of the Landsat satellites with a threshold of zero was found to yield the best results. These bands are typically used to delineate glaciers, but were found to be the most effective in this study particularly when dealing with delineating the boundary of the lake even when large debris-covered icebergs were present near the calving front. It is possible that Imja Tsho being located on a debris-covered glacier may have aided the effectiveness of this particular band combination. Nonetheless, large debris-covered icebergs near the glacier calving front may still cause pixels to be misclassified as land rather than water. These pixels are manually corrected in post-processing. Furthermore, at the calving front it can be difficult to distinguish the lake and icebergs from melt ponds located immediately behind the calving front. To prevent misclassification of the calving front, pixels classified as water that are not cardinally connected to the lake are classified as melt ponds. The perimeter of the lake, which is used to quantify uncertainty, is defined as any water pixel that has a land pixel in any cardinal or diagonal direction. The maximum error associated with the NDWI estimated lake areas is the number of perimeter pixels multiplied by half the area of a pixel, since pixels on the perimeter that are more than half land would be classified as land.

2.3 Calving retreat of Imja-Lhotse Shar Glacier

The calving front was defined in the NDWI image processing as the last pixel in each row that has a lake pixel to its left and a land pixel to its right. A problem arises in the southern-most calving front pixels in which a calving front pixel is defined in a later image, but is not defined in an earlier image because the lake's width expanded. In this circumstance (which occurs three times between the 1992 and 2002 images and two times between the 2002 and 2012 images) the calving front pixel for the older image is considered equal to the closest calving front pixel. The calving rate for a row may then be computed as the difference between calving front pixels within a given row. The maximum error in this calving rate estimate is one pixel.

2.4 Ground penetrating radar survey

In order to better understand the structure of the Imja-Lhotse Shar glacier in the proximity of the eastern end of Imja Tsho, a Ground Penetrating Radar (GPR) survey was conducted there. The transect of the survey is shown in Fig. 2. The equipment for the GPR survey was a custom built, low frequency, short-pulse, ground-based radar system. Gades et al. (2000) used a similar system on the debris-covered Khumbu glacier near Imja Tsho, but it was not configured for moving transects. The GPR transmitter was a Kentech Instruments Ltd. GPR pulser outputting 4 kV signals with a 12 V power source. The receiving antenna is connected to an amplifier and a National Instruments USB-5133 digitizer whose output feeds into a LabView program for immediate processing in the field and correlation with GPS signals. Using a common offset, in-line deployment, the GPR pulses are transmitted and received through 10 MHz weighted dipole antennae threaded inside climbing webbing. Post-processing steps performed on the data included: removal of pre-trigger points; deglitching; demeaning with smoothing of the mean trace; detrending; bandpass filtering; conversion of two-way travel time to depth when radar velocity is available; depth stripping; and normalizing by maximum absolute value.

TCD
8, 2375–2401, 2014

Changes in Imja Tsho in the Mt. Everest region of Nepal

M. A. Somos-Valenzuela et al.

Errors in the GPR measurements arise from two main sources, the selection of the precise bed reflection location, and uncertainty in the radar wave velocity within the glacier (Gades et al., 2000). Errors in selecting the bed location from the data depends on signal frequency and strength of the reflection and generally results in constant uncertainty for all measurements in a profile. The uncertainty in selecting the bed reflection was ±7.5 m, which corresponds to the approximate 15 m vertical width of the reflection. Errors in wave velocity, assumed to be $167 \pm 4 \times 10^6\,\mathrm{m\,s^{-1}}$, result in uncertainty that increases with ice thickness.

3 Results and discussion

3.1 Bathymetric survey

A contour map of the depth of the bottom of Imja Tsho derived from the sonar bathymetric measurements are shown in Fig. 3. Water depths of 20–60 m were measured near the western edge of the lake (outlet end) and 30–100+ m deep near the eastern (glacier) end of the lake. Thick iceberg coverage on the eastern end of the lake prevented transects from being performed up to the calving front. Elevations within the 100 m-contour were interpolated from the surrounding values as previously described. Compared to the 2002 depths, the lake bottom has continued to lower as the ice beneath the lake has melted.

The bathymetric survey results are reported in Table 1, and they show that the volume and depth of Imja Tsho has increased considerably over the last two decades. As a result of the lake expansion and deepening, the estimated volume of water in the lake nearly doubles from the 2002 estimate, i.e., from 35.8 ± 0.7 million $\mathrm{m^3}$ in 2002 to 61.6 ± 1.8 million $\mathrm{m^3}$ in 2012. The accuracy of the 1992 data are unknown; however, Fujita et al. (2009) estimated the uncertainty of the 2002 data to be ±0.7 million $\mathrm{m^3}$ by assuming the depth measurement error to be 0.5 m. The volume of the lake in 2012 was 72 % larger than in 2002, increasing at an average annual rate of

2.58 ± 0.25 million $m^3\,yr^{-1}$. Compared to the prior surveys, the results of this study show that the eastern region of the lake has deepened over the last decade (2002–2012) as the ice beneath has melted, with the average depth increasing by $0.64\pm0.3\,m\,yr^{-1}$ and the maximum depth by $2.58\pm0.08\,m\,yr^{-1}$. Figure 4 shows the 2012 bathymetric survey results along section A-A′ from Fig. 3 along with those of the 1992 and 2002 surveys (Sakai et al., 2003, Fig. 4, p. 559), indicating an eastward expansion of the lake, rapid retreat of the glacier ice cliff and the subaqueous melting that has taken place.

Two distinct zones of Imja Tsho with different depths are illustrated in Fig. 4: zone A, from 0 m to 1000 m on (western part), and zone B, from 1000 m to 2100 m (eastern part). The exact separation between these two zones is unknown, but it is estimated from the bathymetric data to occur at about 1000 m in Fig. 4. Reasons for the differences in depth between the two zones are not entirely clear, but may be related to the presence or lack thereof of ice at the lake bottom. That is, a lack of ice at the bottom of zone A would arrest all further deepening, while the presence of ice at the bottom of zone B would account for its continued deepening. This might also be due to the presence of a thick debris cover on the ice at the bottom of zone A but not in zone B. When the lake grew to form the western part (zone A), the growth rate was smaller; therefore, more debris might have deposited on the lake bottom.

3.2 Areal expansion of Imja Tsho

The NDWI classifications of water pixels for the Landsat images described previously are shown in white in Fig. 5 for 2012. All the images have pixels identified as melt ponds and the 2012 image has debris-covered icebergs in the lake area, both of which are manually corrected for in post-processing. The lake areas derived from the 1992, 2002, and 2012 images are shown in Table 2. The estimated 1992 lake area of $0.648\pm0.073\,km^2$ agrees very well with the $0.60\,km^2$ lake area estimated by Yamada and Sharma (1993) in April 1992. The difference between these two measurements may be due to the lake expansion during the 1992 melt season and/or the error associated with the satellite image. The NDWI estimated 2002 lake area of 0.867 ± 0.091 km^2 also agrees well with the 0.86 km^2 area that Sakai et al. (2003) estimated, although the satellite imagery methods used in the referenced study were not described. The good agreement between the NDWI estimated areas and the previous studies demonstrates the effectiveness of using NDWI to outline the lake. The maximum errors for the three images are shown in Table 2. The areal expansion of Imja Tsho over the last 50 years is shown in Fig. 6. The decadal expansion rate has increased to 0.039 ± 0.0195 km^2 yr^{-1}.

3.3 Calving retreat of Imja-Lhotse Shar Glacier

The areal expansion of Imja Tsho is primarily in the eastward (up-glacier) direction due to the retreat of the calving front. The average calving retreat distances for 1992–2002, 2002–12, and 1992–2012 are shown in Table 3. The average calving retreat increased from 316 ± 201 m during 1992 to 2002 to 526 ± 231 m (max error = 30 m) from 2002 to 2012. The corresponding standard deviations of calving retreat of 201 m and 231 m, respectively during each decade, are large due to the calving front having an arm-like shape in 2002, which caused a non-uniform retreat of the calving front. These calving retreats correspond to calving rates of 32 ± 20 m yr^{-1} and 53 ± 23 m yr^{-1} (max error = 3 m yr^{-1}). The overall calving rate from 1992 to 2012 was 43 ± 8 m yr^{-1} (max error = 3 m yr^{-1}).

3.4 Drainable water from Imja Tsho

Using the bathymetric data reported above, we calculated the volume of water that could drain from Imja Tsho based on various levels of the lake surface. For example, the amount of water that could be drained from the lake is 34.08 ± 0.54 million m^3 if the lake surface elevation decreases 35 m from 5010 m to 4975 m (the elevation of the valley floor below the lake). The previous estimates of this volume were 15 million m^3 (1992) and 21 million m^3 (2002) (Sakai et al., 2003). The 2012 estimate is 40.5 % larger than the 2002 value. If the lake were drained to a water surface elevation higher than the valley floor then the volume would decrease as shown in Fig. 7.

In the event of a breach of the former glacier terminus, water may not drain from the lake all at once and the timing or the hydrograph of the drainage is important in order to estimate the critical water volume that might cause serious damage downstream. However, detailed calculation of the volume and timing of discharge in the event of a breach of Imja Tsho requires extensive numerical simulations and is beyond the scope of this paper. Due to the continued areal expansion of the lake, there is an increasing amount of water that could drain from the lake in the event of a breach; however, this does not necessarily mean that the probability of occurrence of such an event increases.

3.5 GPR survey of Imja-Lhotse Shar Glacier

Figure 8 shows the results of the GPR survey for the transect across the Imja-Lhotse Shar glacier from north to south using a 10 Mhz antenna and assuming a velocity of propogation through the ice of $167 \times 10^{6}\,\mathrm{m\,s^{-1}}$. The thickness of the glacier varies from 40 ± 9.27 to 60 ± 9.27 m thick near the lateral moraines to 217 ± 12.71 m thick in the center of the glacier, significantly below the lake bottom. GPR surveys were also made in the western end of the lake in the moraine region, but the results are still being analyzed. The depth of mixed debris and ice in the western moraine end of the lake are difficult to determine from the GPR results.

4 Conclusions

The results of a 2012 bathymetric survey of Imja Tsho show that the lake has deepened from 98 m to 116±0.25 m between 2002 and 2012. Likewise, the volume has increased from 35.8±0.7 million $\mathrm{m^3}$ to 61.6±1.8 million $\mathrm{m^3}$ over the same period, a 70 % increase. The lake volume is increasing at a rate of 2.58 ± 0.25 million $\mathrm{m^3\,yr^{-1}}$, and the average depth increasing by 0.64 ± 0.3 m yr^{-1}. Our survey results suggest that the lake bottom has continued to lower as the ice beneath it has melted. The lake continues to expand due to the retreat of the glacier terminus (eastern end of the lake) through calving processes. The rate of retreat of the glacier terminus has increased to 53 ± 23 m yr^{-1} over the last decade and the areal expansion rate has increased to 0.039 ± 0.0195 $\mathrm{km}^2\,\mathrm{yr}^{-1}$. The results of the GPR survey for the transect across the Imja-Lhotse Shar glacier show that the ice–bedrock interface is significantly below the lake bottom (perhaps as much as 75 m) with the ice thickness over 217 ± 12.71 m thick in the center of the glacier. The continued expansion of the lake has increased the volume of water that could be released from the lake in the event of a breach in the damming moraine to 34.08 ± 0.54 million m^3, rather than 21 million m^3 estimated in 2002 if the lake surface elevation decreases from 5010 m to 4975 m (the elevation of the valley floor below the lake).

Acknowledgements. The authors acknowledge the support of the USAID Climate Change Resilient Development (CCRD) project, the Fulbright Foundation for the support of Somos-Valenzuela, and the National Geographic Society for their support of Byers. We also acknowledge the support of Dhananjay Regmi of Himalayan Research Expeditions for logistical support during fieldwork, Damodar Lamsal for providing us with a digital elevation model of the Imja Tsho and glacier area, and Alexandra Turney of the University of Texas at Austin in calculating the Imja Lake areas and glacier retreat. The comments of Jack Ives, Elizabeth Byers, and Katalyn Voss are greatly appreciated.

References

Bajracharya, S. R., Mool, P. K., and Shrestha, B. R.: Impact of Climate Change on Himalayan Glaciers and Glacial Lakes: Case Studies on GLOF and Associated Hazards in Nepal and Bhutan, International Centre for Integrated Mountain Development (ICIMOD), Kathmandu, 2007.

Benn, D. I., Bolch, T., Hands, K., Gulley, J., Luckman, A., Nicholson, L. I., Quincey, D., Thompson, S., Toumi, R., and Wiseman, S.: Response of debris-covered glaciers in the Mount

Everest region to recent warming, and implications for outburst flood hazards, Earth-Sci. Rev., 114, 156–174, 2012.

Bolch, T., Buchroithner, M. F., Peters, J., Baessler, M., and Bajracharya, S.: Identification of glacier motion and potentially dangerous glacial lakes in the Mt. Everest region/Nepal using spaceborne imagery, Nat. Hazards Earth Syst. Sci., 8, 1329–1340, doi:10.5194/nhess-8-1329-2008, 2008.

Bolch, T., Pieczonka, T., and Benn, D. I.: Multi-decadal mass loss of glaciers in the Everest area (Nepal Himalaya) derived from stereo imagery, The Cryosphere, 5, 349–358, doi:10.5194/tc-5-349-2011, 2011.

Byers, A. C.: An assessment of contemporary glacier fluctuations in Nepal's Khumbu Himal using repeat photography, Himalayan Journal of Sciences, 4, 21–26, 2007.

Carrivick, J. L. and Rushmer, E. L.: Understanding high-magnitude outburst floods, Geology Today, 22, 60–65, 2006.

Frey, H., Huggel, C., Paul, F., and Haeberli, W.: Automated detection of glacier lakes based on remote sensing in view of assessing associated hazard potentials, in: Proceedings of the 10th International Symposium on High Mountain Remote Sensing Cartography, 8–11 September 2008, Kathmandu, Nepal, edited by: Kaufmann, V. and Sulzer, W., Grazer Schriften der Geographie und Raumforschung, vol. 45, 261–272, 2010.

Fujita, K., Sakai, A., Nuimura, T., Yamaguchi, S., and Sharma, R. R.: Recent changes in Imja Tsho and its damming moraine in the Nepal Himalaya revealed by in-situ surveys and multi-temporal ASTER imagery, Environ. Res. Lett., 4, 045205, doi:10.1088/1748-9326/4/4/045205, 2009.

Gades, A., Conway, H., and Nereson, N.: Radio echo-sounding through supraglacial debris on Lirung and Khumbu Glaciers, Nepal Himalayas, in: Proceedings of Debris-Covered Glaciers, edited by: Nakawo, M., Raymond, C. F., and Fountain, A., Seattle, September 2000, IAHS Publ. no. 264, 13–22, 2000.

Gardelle, J., Arnauda, Y., and Berthier, E.: Contrasted evolution of glacial lakes along the Hindu Kush Himalaya mountain range between 1990 and 2009, Global Planet. Change, 75, 47–55, 2011.

Hagen, T., Dyrenfurth, G. O., von Fiirer-Haimendorf, C., and Schneider, E.: Mount Everest: Formation, Population and Exploration of the Everest Region, Oxford University Press, London, 1963.

Hambrey, M. J., Quincey, D. J., Glasser, N. F., Reynolds, J. M., Richardson, S. J., and Clemmens, S.: Sedimentological, geomorphological and dynamic context of debris-mantled glaciers, Mountain Everest (Sagarmatha) region, Nepal, Quaternary Sci. Rev., 27, 2361–2389, 2008.

Hammond, J. E.: Glacial Lakes in the Khumbu Region, and Nepal: An Assessment of the Hazards, M.A. Thesis, University of Colorado, Boulder, CO, 1988.

Ives, J. D., Shrestha, R. B., and Mool, P. K.: Formation of Glacial Lakes in the Hindu Kush-Himalayas and GLOF Risk Assessment, International Centre for Integrated Mountain Development (ICIMOD), Kathmandu, 2010.

Jianchu, X., Shrestha, A., Vaidya, R., Eriksson, M., and Hewitt, K.: The Melting Himalayas: Regional Challenges and Local Impacts of Climate Change on Mountain Ecosystems and Livelihoods, ICIMOD Technical Paper, International Centre for Integrated Mountain Development (ICIMOD), Kathmandu, 2007.

Lamsal, D., Sawagaki, T., and Watanabe, T.: Digital terrain modelling using Corona and ALOS PRISM data to investigate the distal part of Imja-Lhotse Shar glacier, Khumbu Himal, Nepal, J. Mt. Sci., 8, 390–402, 2011.

McFeeters, S.: The use of the normalized difference water index (NDWI) in the delineation of open water features, Int. J. Remote Sens., 17, 1425–1432, 1996.

Mool, P. K., Bajracharya, S. R., and Joshi, S. P.: Inventory of Glaciers, Glacial Lakes and Glacial Lake Outburst Floods: Monitoring and Early Warning Systems in the Hindu Kush-Himalayan Region, Nepal, International Centre for Integrated Mountain Development (ICIMOD), Kathmandu, 2001.

Nuimura, T., Fujita, K., Yamaguchi, S., and Sharma, R. R.: Elevation changes of glaciers revealed by multitemporal digital elevation models calibrated by GPS survey in the Khumbu region, Nepal Himalaya, 1992–2008, J. Glaciol., 58, 648–656, doi:10.3189/2012JoG11J061, 2012.

Quincey, D. J., Richardson, S. D., Luckman, A., Lucas, R. M., Reynolds, J. M., Hambrey, M. J., and Glasser, N. F.: Early recognition of glacial lake hazards in the Himalaya using remote sensing datasets, Global Planet. Change, 56, 137–152, 2007.

Robertson, C. M., Benn, D. I., Brook, M. S., Fuller, I. C., and Holt, K. A.: Subaqueous calving margin morphology at Mueller, Hooker and Tasman glaciers in Aoraki/Mount Cook National Park, New Zealand, J. Glaciol., 58, 1037–1046, doi:10.3189/2012JoG12J048, 2012.

Sakai, A., Fujita, K., and Yamada, T.: Volume Change of Imja Tsho in the Nepal Himalayas, Disaster Mitigation and Water Management, 7–10 December ISDB 2003, Niigate, Japan, 2003.

Shrestha, A. B. and Aryal, R.: Climate change in Nepal and its impact on Himalayan glaciers, Reg. Environ. Change, 11, S65–S77, doi:10.1007/s10113-010-0174-9, 2011.

UNDP – United Nations Development Programme: Community Based Glacier Lake Outburst and Flood Risk Reduction in Nepal, Project Document, UNDP Environmental Finance Services, Kathmandu, Nepal, 2013.

USACE – United States Army Corps of Engineers: Uncertainty in Bathymetric Surveys, Coastal and Hydraulics Engineering Technical Note ERDC/CHL CHETN-IV-59, Vicksburg, MS, 2003.

Watanabe, T., Ives, J. D., and Hammond, J. E.: Rapid growth of a glacial lake in Khumbu Himal, Himalaya: prospects for a catastrophic flood, Mt. Res. Dev., 14, 329–340, 1994.

Watanabe, T., Kameyama, S., and Sato, T.: Imja-Lhotse Shar glacier dead-ice melt rates and changes in a supra-glacial lake, 1989–1994, Khumbu Himal, Nepal: danger of lake drainage, Mt. Res Dev., 15, 293–300, 1995.

Watanabe, T., Lamsal, D., and Ives, J. D.: Evaluating the growth characteristics of a glacial lake and its degree of danger of outburst flooding: Imja-Lhotse Shar glacier, Khumbu Himal, Nepal, Norsk Geogr. Tidsskr., 63, 255–267, 2009.

Yamada, T. and Sharma, C. K.: Glacier Lakes and Outburst Floods in the Nepal Himalaya, in Snow and Glacier Hydrology, in: Proc., Kathmandu Symposium, 16–21 November, IAHS Publication No. 218, Oxfordshire, UK, 1993.

Title Page
Abstract | Introduction
Conclusions | References
Tables | Figures
◀| |▶
◀ ▶
Back | Close
Full Screen / Esc
Printer-friendly Version
Interactive Discussion

Table 1. Comparison of Imja Tsho 2012 Bathymetric Survey Results with previous studies.

Study	No. of measurement points	Volume (10^6 m^3)	Average Depth (m)	Maximum Depth (m)
1992 (Yamada and Sharma, 1993)	61	28.0	47.0	98.5
2002 (Sakai et al., 2003)	80	35.8 ± 0.7	41.6 ± 0.5	90.5 ± 0.5
2012 (This study)	10 020	61.6 ± 1.8	48 ± 2.5	116.3 ± 0.25

Table 2. Imja Tsho Area Expansion 1992–2012.

Year	Icebergs (no.)	Melt Ponds (no.)	Lake Pixels (no.)	Perimeter Pixels (no.)	Area (km^2)	Max. Error (km^2)	Decade Expansion Rate ($km^2 yr^{-1}$)	Max. Error ($km^2 yr^{-1}$)
1992[1]					0.60			
1992[3]	0	12	720	162	0.648	0.073		
2002[2]					0.868	0.037	0.026	
2002[3]	0	28	963	202	0.867	0.091	0.022	0.0128
2012[3]	15	2	1397	231	1.257	0.104	0.039	0.0195

[1] Yamada and Sharma (1993),

[2] Fujita et al. (2009, Table 1, p. 2),

[3] This study.

Table 3. Calving retreat of Imja-Lhotse Shar Glacier for 1992–2012 based on landsat images.

Period	Calving Retreat Average (m)	Std. Dev. (m)	Max. Error (m)	Calving Rate ($\mathrm{m\,yr^{-1}}$)
1992–2002	316	201	30	31.6
2002–2012	526	231	30	52.6
1992–2012	861	83	30	43.0

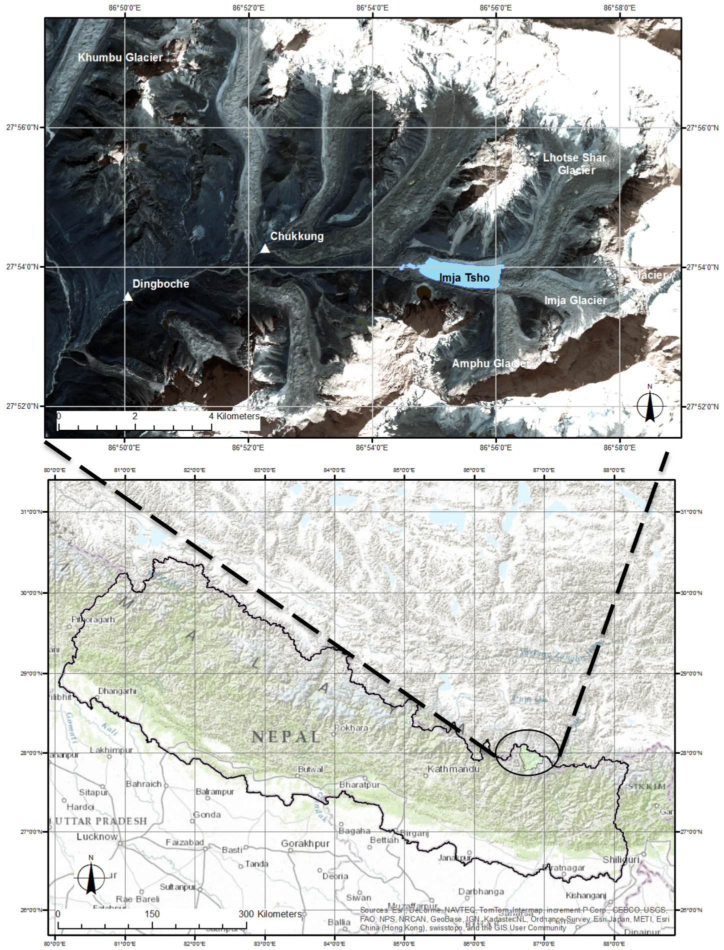

Fig. 1. Location of the Imja Tsho in the Khumbu region of Nepal.

Title Page
Abstract
Introduction
Conclusions
References
Tables
Figures
◀|
|▶
◀
▶
Back
Close
Full Screen / Esc
Printer-friendly Version
Interactive Discussion

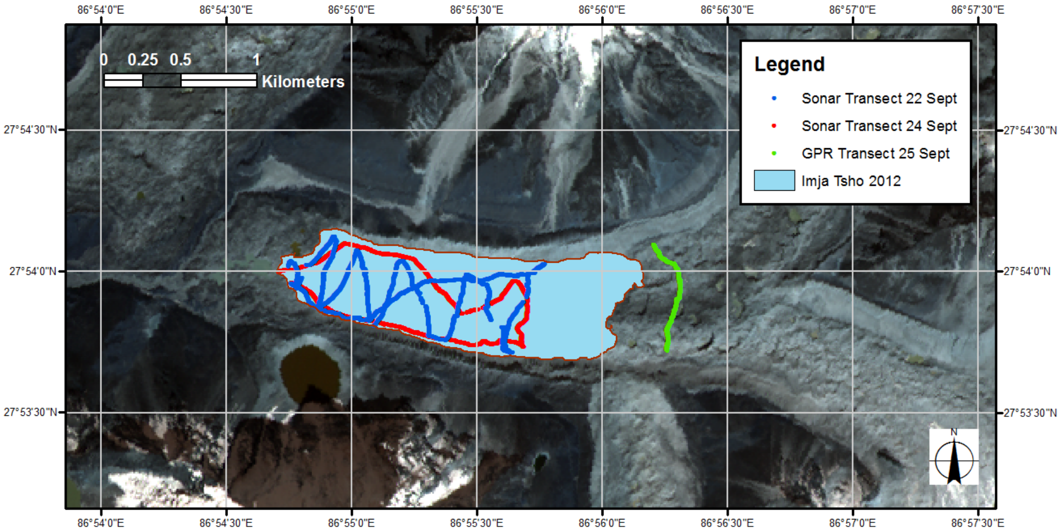

Fig. 2. Sonar bathymetric survey transects at Imja Tsho 22 September (red) and 24 (blue), and the GPR transect at Imja-Lhotse Shar glacier 25 September (green). The background is an ALOS image from 2008.

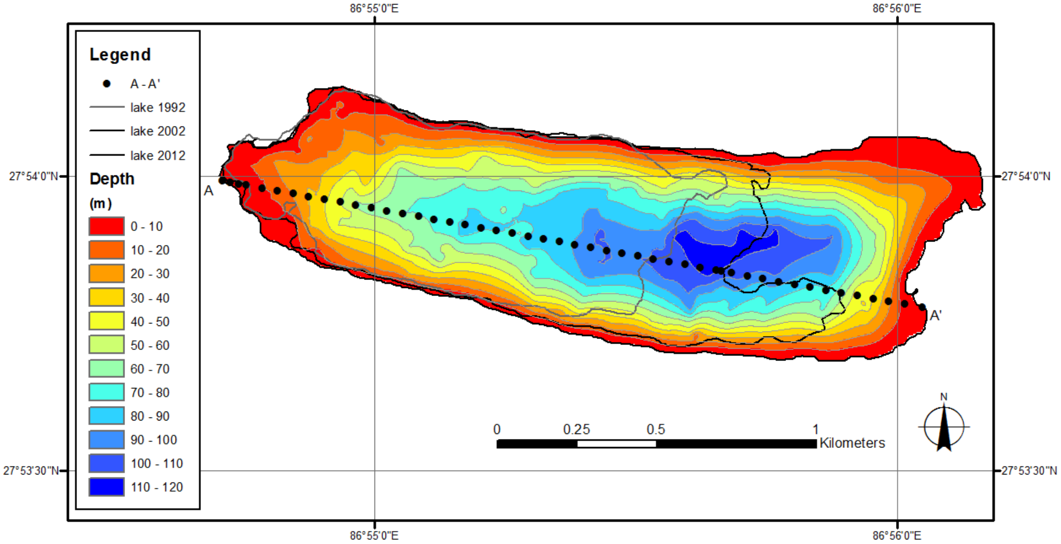

Fig. 3. Bathymetric survey results from Imja Tsho in September 2012.

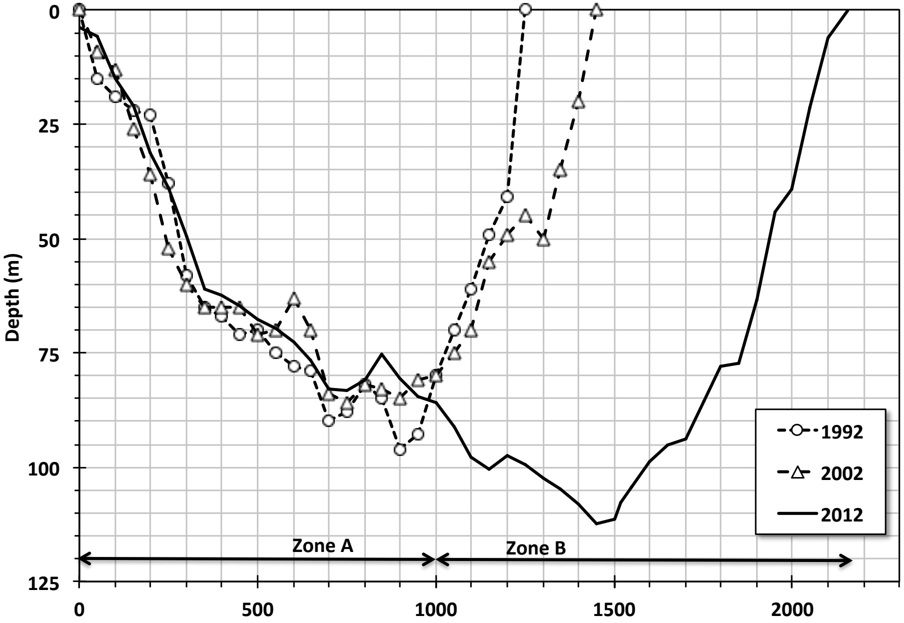

Fig. 4. Cross-section A-A′ of 2012 bathymetric survey data for Imja Tsho compared to 1992 and 2002 surveys.

Title Page
Abstract
Introduction
Conclusions
References
Tables
Figures
I◀
▶I
◀
▶
Back
Close
Full Screen / Esc
Printer-friendly Version
Interactive Discussion

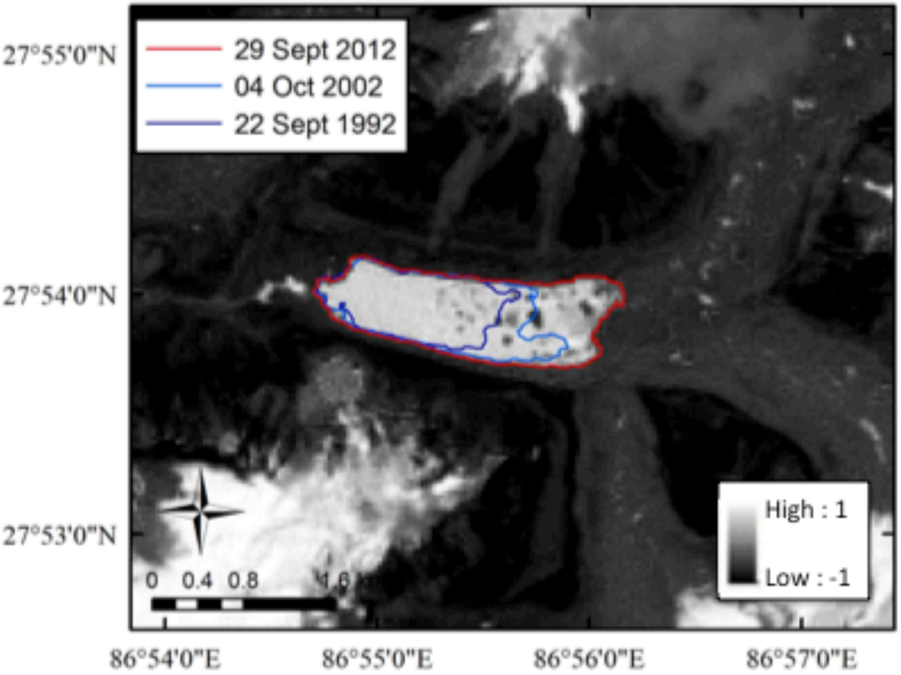

Fig. 5. NDWI calculated from Landsat images for 2012.

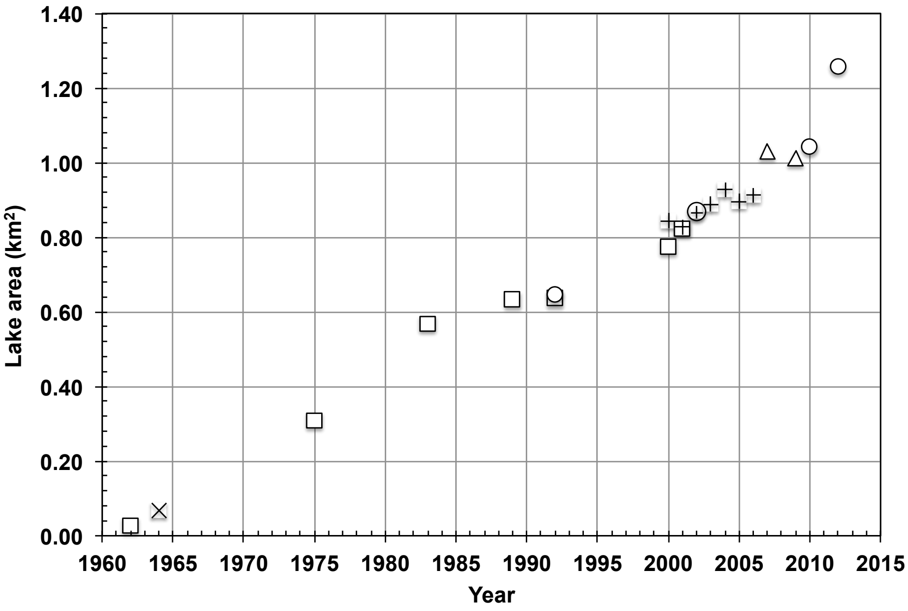

Fig. 6. Imja Tsho Area Expansion 1962–2012 (Source: □ – Bajracharya et al. (2007); ◊ – Yamada and Sharma (1993); + – Fujita et al. (2009); × – Lamsal et al. (2011); △ – Watanabe et al. (2009); and ◯ – this study).

Title Page
Abstract | Introduction
Conclusions | References
Tables | Figures
◂◂ | ▸▸
◂ | ▸
Back | Close
Full Screen / Esc
Printer-friendly Version
Interactive Discussion

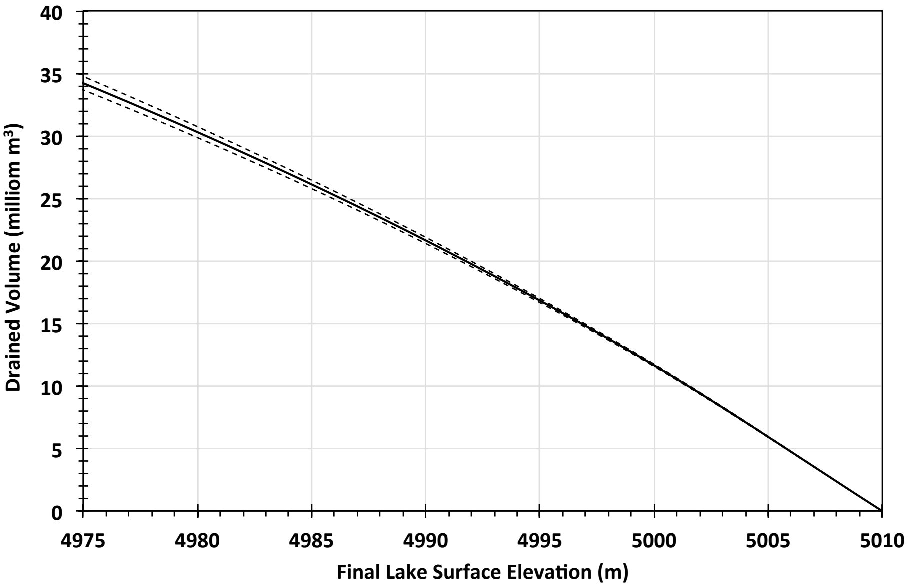

Fig. 7. Potentially drained volume from Imja Tsho vs. lake surface elevation. Dashed lines show the calculated drained volume plus or minus one standard deviation.

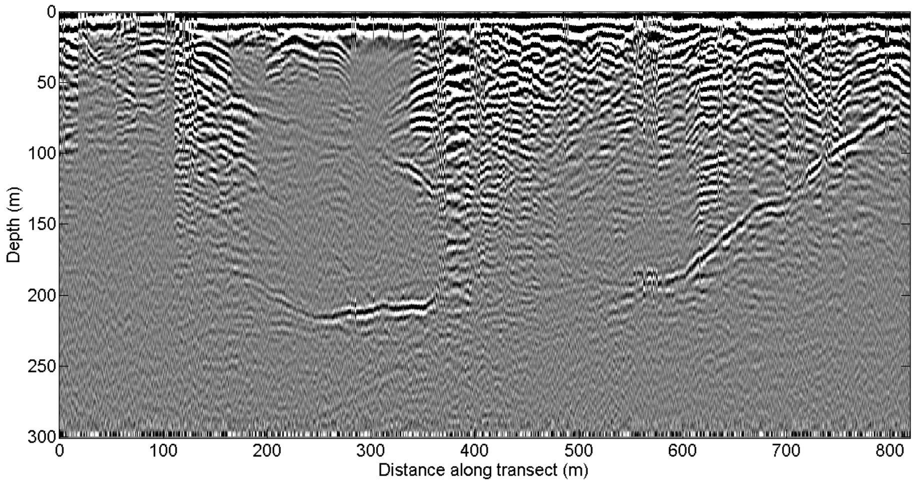

Fig. 8. GPR transect across Imja/Lhotse Shar glacier from north to south on 25 September 2012 using a 10 MHz antenna and velocity in ice of 167 × 10^6 m s^{-1}.